

Diffusion-weighted magnetic resonance imaging in the early detection of tumour response to therapy

Nick J.F. Dodd¹, S. Zhao² and J.V. Moore¹

¹Paterson Institute for Cancer Research and ²North West Medical Physics, Christie Hospital (NHS) Trust, Manchester, United Kingdom

Early detection of the effects of therapy offers distinct clinical advantages for the management of the patient, since the response of a tumour to a particular therapy may vary considerably from patient to patient. A pre-clinical tumour model was used to study the effects of two novel therapies, photodynamic therapy and electrotherapy, in addition to a well established modality, radiotherapy. In each case, diffusion-weighted magnetic resonance imaging was found to be of value in determining the therapeutic response, within two days of treatment. Following photodynamic therapy, the apparent diffusion coefficient (ADC) of water in those regions of the tumour that became necrotic showed a marked increase within one day of treatment, while no significant increase was detectable in those regions that remained viable. A similar increase in ADC was observed following electrotherapy, whether anodic or cathodic, the increase being detected within minutes of treatment in the regions of primary damage and within about one day in the regions of secondary ischaemic necrosis. The changes produced by radiotherapy were less marked than those produced by the other therapies, but, following doses that produce a high proportion of killing, there was a statistically significant increase in ADC within one or two days of treatment.

Key words: neoplasms, experimental-therapy; photodynamic therapy; electric stimulation therapy; radiotherapy; magnetic resonance imaging

Introduction

The ability to monitor non-invasively and at early times, the cytotoxic effects of cancer treatment in an individual subject is potentially of great clinical value. This is particularly true of new forms of therapy, where the

response of a specific tumour type to a standard treatment regime may not have been extensively studied. Photodynamic therapy (PDT) involves injection of a non-toxic photosensitizing drug, followed by exposure to visible light at non-thermal levels. The extent of tumour destruction produced by a given dose of photosensitizer and incident light is strongly influenced by the biodistribution of the drug and absorption of light within the tumour and in surrounding tissue.¹ In the case of electrotherapy, our preliminary stud-

Correspondence to: Dr. N.J.F. Dodd, Paterson Institute for Cancer Research, Christie Hospital (NHS) Trust, Manchester M20 9BX, UK. Tel: +44-161-446 3151; Fax: +44-161-446 3109; E-mail: ndodd@picr.man.ac.uk

ies²⁻⁴ suggest that the efficacy of the treatment may be strongly influenced by precise placement of the electrodes and the vascular architecture of the tumour. Consequently considerable inter-patient variability in tumour response to therapy may occur. This is observed even in a well established treatment such as radiotherapy, where the outcome is influenced by intrinsic radiosensitivity of the tumour cells and the hypoxic fraction.

Proton MRI offers a potential method for non-invasive monitoring of the efficacy of cancer treatment. Our previous studies^{1,5} using an experimental mammary (T50/80) tumour have shown that, within 24 h of PDT, regions of high signal intensity in a T_2 -weighted image correlated well with histological necrosis. Moreover, using MRI to assess the proportion by volume of the tumour tissue destroyed by treatment, this correlated with the subsequent delay in tumour regrowth. Further studies,⁶ using the AT6/22 prostate tumour, showed that T_2 -weighted images taken 24 h after PDT similarly demonstrated the presence of treatment-induced necrosis as areas of hyperintensity. However, the contrast between viable and necrotic regions was less marked than previously observed in the mammary tumour model. In both tumour models, differences between T_2 (and T_1) of viable tumour tissue and treatment-induced necrosis were of the same order as variations between individual tumours and could not be used as a reliable marker of tissue state. We show here that MR measurement of the apparent diffusion coefficient (ADC) of tumour water provides a quantitative marker of PDT-induced necrosis both for the mammary tumour⁷ and also for the prostate tumour⁶ although the untreated tumours show markedly different absolute values of ADC.

The effects of electrotherapy on the mouse mammary tumour⁴ and on normal rat liver³ have been detected by T_2 -weighted MR images, but the effects of radiotherapy are

reported to produce little or no significant changes in the T_1 - or T_2 -weighted images of animal tumours⁸⁻¹⁰ or human brain tumours.¹¹ The effects of radiotherapy are normally only detected by MRI at a late stage, when changes in tumour volume can be readily observed. We have now applied the diffusion method to monitoring the early effects of PDT, electrotherapy and radiotherapy in our experimental systems.

Materials and methods

The tumours were a T50/80 mouse mammary tumour¹² and a Dunning rat AT6/22 prostate tumour, both implanted subcutaneously in nude, immune-suppressed mice. The tumours were treated with photodynamic therapy, electrotherapy or radiotherapy when they reached a volume $>600 \text{ mm}^3$. PDT involved i.p. injection of 40 mg kg^{-1} of haematoporphyrin esters in saline, followed 24 h later by illumination with 630 nm light at 100 mW cm^{-2} from a laser, to a dose of $80\text{--}150 \text{ J cm}^{-2}$. Electrotherapy involved insertion of a gold needle electrode into the tumour while the animal lay on a copper plate counter-electrode, covered with a conducting gel (Dracard, Maidstone, UK) and a current of 5 mA was passed for 15–30 min. For radiotherapy, tumours were exposed to 300 kV X-rays at a dose rate of 4 Gy min^{-1} , to a dose of 30 Gy, while the bulk of the animal was protected by a lead shield.

Magnetic resonance imaging was performed with a 4.7 T Biospec system. Proton images were acquired with a 2.5 cm diameter surface coil. For diffusion measurements, a pair of gradients of maximum amplitude 20 mT m^{-1} and duration 20 ms, separated by 12 ms were used. This gave a maximum gradient factor, b , of $0.68 \times 10^9 \text{ s m}^2$. The apparent diffusion coefficient of the tumour water in each region (D_i) was calculated by the method of Le Bihan *et al.*¹³, using the formula:

$$D_i = \ln[S_0/S_1]/[b_1 - b_0]$$

where S_0 and S_1 are the signal intensities measured with gradient factors b_0 and b_1 respectively.

Results

Photodynamic therapy

The ADC of water in the untreated mammary tumour was approximately half that in the prostate tumour (T50/80: $D = 0.23 \pm 0.02 \times 10^{-9} \text{ m}^2\text{s}^{-1}$; AT6/22: $D = 0.61 \pm 0.03 \times 10^{-9} \text{ m}^2\text{s}^{-1}$). However, following PDT of either tumour type, the ADC in those regions of the tumour that became necrotic showed a marked increase ($p < 0.0001$), within 1 day of treatment (T50/80: $D = 1.04 \pm 0.03 \times 10^{-9} \text{ m}^2\text{s}^{-1}$; AT6/22: $D = 1.23 \pm 0.06 \times 10^{-9} \text{ m}^2\text{s}^{-1}$), while showing no significant increase in those regions that remained viable (Figure 1). Subsequent histological examination of the tumours confirmed the assignments based on ADC increase.

Electrotherapy

The magnitude of the changes in ADC observed following electrotherapy, either anodic or cathodic (Table 1), were found to be similar to those induced by PDT. In contrast, the timescale of development of damage was different. Primary damage, occurring symmetrically around the implanted electrode, was detectable by MRI or by histology within minutes of treatment. In some tumours treated by electrotherapy, secondary ischaemic damage appeared approximately 1 day after treatment (Figure 2). This latter type of damage was similar in nature to the PDT-induced damage. Both types of electrotherapy-induced damage were clearly delineated by the increased ADC and were distinguished from one another by their different rates of development.

Radiotherapy

The changes produced by radiotherapy were less marked than those produced by PDT or electrotherapy, but, following doses that produce a high proportion of cell killing (e.g. 30

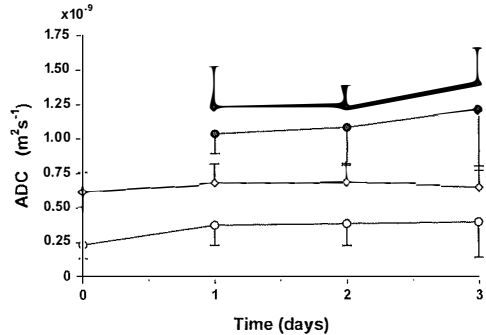


Figure 1. Changes in tumour water ADC with time after photodynamic therapy, in T50/80 mammary tumours (○, ●) ($n=16$) and AT6/22 prostate tumours (◇, ◆) ($n=22$), showing mean and standard error. The open symbols denote viable tumour tissue and the closed symbols denote necrotic tissue.

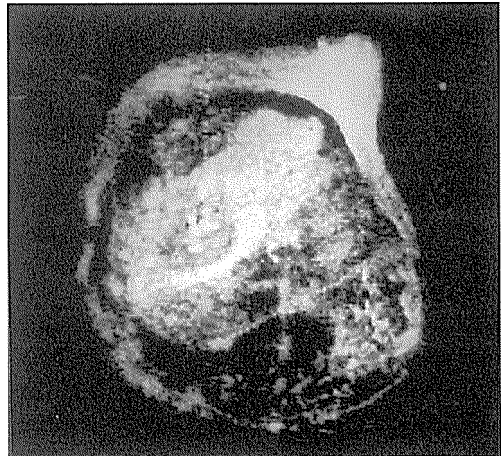
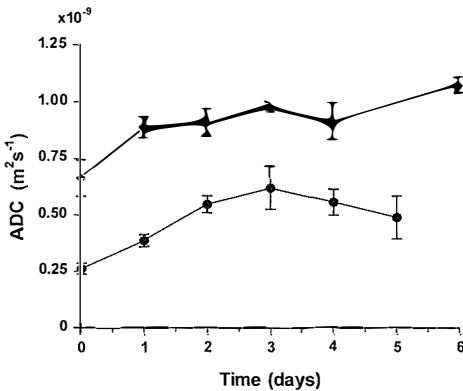


Figure 2. Proton magnetic resonance image of a T50/80 tumour, one day after electrotherapy with a gold needle anode in the tumour and a current of 5 mA passed for 30 minutes. The image shows a hyperintense ring of dermal oedema around the tumour (particularly thickened at the upper right hand edge), a diffuse circular area within the tumour (slightly left of centre) representing the primary necrotic damage and an approximately oval hyperintense region of secondary ischaemic necrosis (from the left hand edge to top right) that was not observable immediately after electrotherapy.

Table 1. ADC of tumour water in different regions of T50/80 mammary and AT6/22 prostate tumours after electrotherapy

Tumour	Viable tissue D x 10 ⁹ (m ² s ⁻¹)	1° damage D x 10 ⁹ (m ² s ⁻¹)	2° damage D x 10 ⁹ (m ² s ⁻¹)
T50/80	0.33±0.02 (n=30)	1.00±0.06 (n=13)	1.25±0.06 (n=4)
AT6/22	0.58±0.04 (n=9)	1.04±0.10 (n=6)	

Gy), there was a small, but statistically significant, increase in ADC within 1 or 2 days of treatment. Comparing the two tumour types (Figure 3), it can be seen that the ADC of the irradiated mammary tumour increased to approximately the value observed in the unirradiated prostate tumour. Experiments currently in progress suggest that the increase in ADC may be proportional to the extent of cell killing, as measured by tumour growth delay.

**Figure 3.** Changes in tumour water ADC with time after radiotherapy (30 Gy) in T50/80 (●) (n=12) and AT6/22 tumours (◆) (n=10), showing mean and standard error.

Discussion

It has previously been reported^{14,15} that when cells are degraded, as in the necrotic regions of a tumour, this region shows a greater ADC than the viable tissue. *In vivo*, the principal mode of action of PDT is believed to be acute injury to the vasculature, with vascular collapse leading to prompt and massive secondary ischaemic necrosis, detectable histologically at about 24 h after treatment. Con-

sistent with this effect, we have observed an increase in tumour water ADC in the regions of PDT-induced necrosis, within about 24 h of treatment, irrespective of the initial value of the ADC in the untreated tumour. We have previously shown³ that secondary ischaemic necrosis is also induced by electrotherapy in normal rat liver and have now shown that it also occurs in some of our experimental tumours. However, the irregular nature of the tumour vasculature and the possibility of collateral blood flow results in less predictable secondary damage than in highly organized liver tissue. The primary necrosis induced by electrotherapy is detectable immediately after treatment and, like the secondary necrosis, causes a significant increase in ADC. Consequently, diffusion-weighted MRI and measurement of ADC provide qualitative and quantitative delineation of the extent of necrosis induced by PDT or by electrotherapy. This non-invasive technique may be invaluable in the management of patients by these new forms of therapy and assist in their clinical acceptance. Towards this aim, we have demonstrated that PDT-induced necrosis can be detected in our experimental tumour models using a mid-field whole-body clinical MR scanner¹⁶.

The effects of ionizing radiation are more diffuse than those of PDT and electrotherapy. Consequently they are more difficult to detect. Although radiotherapy is a well established and widely used mode of therapy, the earliest indication that a tumour has responded to treatment is normally a reduction in volume or slowing of the growth rate. This can be detected by conventional imaging techniques. However, diffusion-weighted

MRI may provide a much earlier indication of treatment efficacy, thereby allowing the radiation dose to be optimized at an early stage during a course of treatment. Although the results presented above are for a single high dose of radiation, we have demonstrated similar changes in ADC during more clinically relevant fractionated doses,¹⁷ to these experimental tumours. Experiments are currently in progress to seek a correlation between change in ADC and biological endpoint, e.g. tumour growth delay.

Increases in ADC have recently been reported in experimental tumours treated with gene therapy¹⁸ and also with cyclophosphamide,¹⁹ 5-fluorouracil^{20,21} or 1,3-bis(2-chloroethyl)-1-nitrosourea,²² in which cases the maximum relative increase in tumour water ADC appeared to be related to therapeutic response. Diffusion-weighted magnetic resonance imaging appears highly promising in the early detection of tumour response to a wide range of treatment modalities.

Acknowledgement

The expert technical assistance of Mr. D. Broadbent is gratefully acknowledged. Financial support was provided by the Cancer Research Campaign and, in part, by the North Western Regional Health Authority.

References

- Moore JV, Dodd NJF, Wood B. Proton nuclear magnetic resonance imaging as a predictor of the effects of photodynamic therapy. *Br J Radiol* 1989; **62**: 869-70.
- Griffin DT, Dodd NJF, Moore JV, Pullan BR, Taylor TV. The effects of low-level direct current therapy on a preclinical mammary carcinoma: tumour regression and systemic biochemical sequelae. *Br J Cancer* 1994; **69**: 875-8.
- Griffin DT, Dodd NJF, Zhao S, Pullan BR, Moore JV. Low-level direct electrical current therapy for hepatic metastases. I. Preclinical studies on normal liver. *Br J Cancer* 1995; **72**: 31-4.
- Dodd NJF, Moore JV, Taylor TV, Zhao S. Preliminary evaluation of low-level direct current therapy using magnetic resonance imaging and spectroscopy. *Phys Medica* 1993; **9**: 285-9.
- Dodd NJF, Moore JV, Poppitt DG, Wood B. *In vivo* magnetic resonance imaging of the effects of photodynamic therapy. *Br J Cancer* 1989; **60**: 164-7.
- Dodd NJF, Lee LK, Moore JV, Zhao S. MRI monitoring of the effects of photodynamic therapy on prostate tumours. *Proceedings 3rd Annual Meeting Soc Magn Reson Med* 1995, 1368.
- Zhao S, Dodd NJF, Moore JV. Magnetization transfer and diffusion in mouse mammary tumours following photodynamic therapy. *Proceedings 2nd Annual Meeting Soc Magn Reson Med* 1994, 1043.
- Bakker CJG, Vriend J. Proton spin-lattice relaxation studies of tissue response to radiotherapy in mice. *Phys Med Biol* 1983; **28**: 331-40.
- Kroeker RM, Stewart CA, Bronskill MJ, Henkelman RM. Continuous distributions of NMR relaxation times applied to tumours before and after therapy with x-rays and cyclophosphamide. *Magn Reson Med* 1988; **6**: 24-36.
- Le Moyec L, Pellen P, Merdrignac-Le Noan G, Le Lan J, Chenal C, de Certaines JD. Proton NMR relaxation times of experimental Lewis lung carcinoma after irradiation. *Radiother Oncol* 1988; **13**: 1-8.
- Houdek PV, Landy HJ, Quencer RM, Sattin W, Poole CA, Green BA, Harmon CA, Pisciotto V, Schwade JG. MR characterization of brain and brain tumour response to radiotherapy. *Int J Radiat Oncol Biol Phys* 1988; **15**: 213-8.
- Moore JV. The dynamics of tumour cords in an irradiated mouse mammary carcinoma with a large hypoxic cell component. *Jpn J Cancer Res* 1988; **79**: 236-43.
- Le Bihan D, Breton E, Lallemand D, Grenier P, Cabanis E, Laval-Jeantet M. MR imaging of intravoxel incoherent motions: application to diffusion and perfusion in neurological disorders. *Radiology* 1986; **161**: 401-7.
- Henkelman RM. Diffusion-weighted MR imaging: a useful adjunct to clinical diagnosis or a scientific curiosity? *Am J Roent* 1990; **155**: 1066-8.
- Maier CF, Paran Y, Bendel P, Rutt BK, Degani H. Quantitative diffusion imaging in implanted human breast tumours. *Magn Reson Med* 1997; **37**: 576-81.
- Dodd NJF, Zhu XP, Dobson MJ, Watson Y, Hawnaur JM, Adams JE. Application of high resolution diffusion imaging in the early detection of tumour response to photodynamic therapy using a 0.5 Tesla conventional whole body MR scanner.

- 5th. Meeting ISMRM, Vancouver. *Proceedings* 1997, 1073.
17. Dodd NJF, Zhao S. Early detection of tumour response to radiotherapy using MRI. *Phys Medica* 1997; 13 (Suppl. 1): 56-60.
18. Poptani H, Ollikainen A, Gröhn O, Kainulainen R, Ylä-Herttua S, Kauppinen R. 5th. Meeting ISMRM, Vancouver. *Proceedings* 1997, Monitoring the efficacy of gene therapy in experimental rat glioma: serial T_2 and diffusion weighted MRI study. 1071.
19. Zhao M, Pipe JG, Bonnett J, Evelhoch JL. Early detection of treatment response by diffusion-weighted $^1\text{H-NMR}$ spectroscopy in a murine tumour in vivo. *Br J Cancer* 1996; 73: 61-4.
20. Zhao M, Evelhoch. Relationship between 5-fluorouracil- or cyclophosphamide-induced changes in tumor apparent diffusion coefficient and therapeutic response in three murine tumours. 5th. Meeting ISMRM, Vancouver. *Proceedings* 1997, 1074.
21. Lemaire L, Howe LA, Rodrigues L, Griffiths JR. In vivo assessment of primary mammary rat tumours response to chemotherapy using diffusion-weighted $^1\text{H-NMR}$ spectroscopy. 5th. Meeting ISMRM, Vancouver. *Proceedings* 1997, 1070.
22. Ross BD, Zhao J, Ercolani M, Ben-Joseph O, Stegman LD, Chenevert TL. Noninvasive quantitation of chemotherapeutic cell kill in experimental intracranial brain tumours using MRI: correlation with changes in diffusion MRI. 5th. Meeting ISMRM, Vancouver. *Proceedings* 1997, 1072.